Protein Engineering, Design & Selection vol. 25 no. 10 pp. 631–638, 2012
Published online August 31, 2012 doi:10.1093/protein/gzs054

Improved drug-like properties of therapeutic proteins by directed evolution

Andrew Buchanan[1], Franco Ferraro, Steven Rust, Sudharsan Sridharan, Ruth Franks, Greg Dean, Matthew McCourt, Lutz Jermutus and Ralph Minter

MedImmune Research, Granta Park, Cambridge CB21 6GH, UK

[1]To whom correspondence should be addressed.
E-mail: buchanana@medimmune.com

Received May 25, 2012; revised May 25, 2012; accepted August 6, 2012

Edited by Andreas Plueckthun

Many natural human proteins have functional properties that make them useful as therapeutic drugs. However, not all these proteins are compatible with large-scale manufacturing processes or sufficiently stable to be stored for long periods prior to use. In this study, we focus on small four-helix bundle proteins and employ ribosome display in conjunction with three parallel selection pressures to favour the isolation of variant proteins with improved expression, solubility and stability. This *in vitro* evolution strategy was applied to two human proteins with known drug development issues, granulocyte colony-stimulating factor (G-CSF) and erythropoietin (EPO). In the case of G-CSF, the soluble expression levels in *Escherichia coli* were improved 1000-fold, while for EPO the level of aggregation in an accelerated shelf-life study was reduced from over 80% to undetectable levels. These results exemplify the general utility of our *in vitro* evolution strategy for improving the drug-like properties of therapeutic proteins.

Keywords: developability/directed evolution/expression/ribosome display/stability

Introduction

Proteins have evolved in nature to fulfil a defined *in vivo* function. However, they have not evolved for use as therapeutic drugs, which present unique challenges such as the need for high stability and expression levels. Although many natural proteins have been developed successfully as therapeutics, there are numerous examples of difficulties encountered during the development process. Granulocyte colony-stimulating factor (G-CSF), which stimulates the production of white blood cells, is used as a treatment to accelerate recovery from neutropaenia in patients after chemotherapy treatment. However, it cannot be expressed solubly in *Escherichia coli* and therefore needs to be refolded from inclusion bodies, requiring a more complicated and expensive manufacturing process. Erythropoietin (EPO), which increases red blood cell (RBC) production, is an approved treatment for anaemia and is normally produced solubly in mammalian cell cultures. However, EPO is a thermodynamically unstable protein that is prone to aggregation at elevated temperatures and has an unstable intermediate species (Arakawa *et al.,* 2001; Banks *et al.,* 2009). In addition, the aggregation of EPO is one of the factors implicated in EPO-derived immunogenicity that caused pure red cell applasia incidents with disastrous consequences (Schellekens and Jiskoot, 2006).

The challenge of improving the stability and expression levels of proteins relates to the process of folding. Protein folding is a reversible process from the unfolded state via intermediates to the fully folded state and stability is dependent upon both the thermodynamic and kinetic properties of the intermediate and fully folded state. As the protein folds and unfolds there is the potential for off-pathway events that result in exposure of hydrophobic patches, aggregation and protein degradation (Baneyx, 1999; Chi *et al.,* 2003; Manning *et al.,* 2010). Since the folding process is linked to the primary polypeptide sequence it is theoretically possible to rationally predict stabilising mutations based on structural or sequence analysis but this has previously been challenging and may compromise function (Lehmann and Wyss, 2001; Tokuriki and Tawfik, 2009).

The more empirical approach of directed evolution has also been used, though rarely for therapeutic proteins, and is often combined with a display technology in order to explore large libraries of variants for improved properties (reviewed in Roodveldt *et al.,* 2005; Manning *et al.,* 2010; Magliery *et al.,* 2011). Yeast display was originally suggested to have an intrinsic ability to select more stable proteins because during yeast secretion the endoplasmic reticulum is thought to provide a quality control step to eliminate poorly folded proteins (Shusta *et al.,* 1999). However, the general utility of this method was questioned in a later study, which suggested that yeast display may identify proteins that are thermodynamically stable and yet still poorly folded and therefore still at risk of aggregation (Park *et al.,* 2006). Phage display combined with thermal denaturation has also been shown to yield proteins with improved aggregation resistance (Jespers *et al.,* 2004). However, a fully *in vitro* method such as ribosome display offers the potential for more precise control over the protein folding conditions. Ribosome display is a cell-free display method that has been used to optimise the affinity and stability of functional proteins (Hanes and Plückthun, 1997; Jermutus *et al.,* 2001; Thom *et al.,* 2006). It can be used in conjunction with various selection pressures such as hydrophobic interaction chromatography matrices (HIC) in order to preferentially isolate protein variants with improved folding properties (Keefe and Szostak, 2001; Matsuura and Plückthun, 2003).

In this paper, we focus on two therapeutic proteins with known drug development issues, G-CSF and EPO. The aim was to extend the utility of ribosome display for stability

selection of therapeutic proteins based on protein folding and function. To create a robust stability selection pressure three factors have been combined for the first time to destabilise proteins, the reducing agent dithiothreitol (DTT), elevated temperature and HIC matrices. A molecule can only survive the selection process if it can fold correctly in these conditions and bind its cognate partner.

Materials and methods

Ribosome display

The DNA construct used for ribosome display, and the assembly by polymerase chain reaction (PCR) have been described in detail previously (Hanes *et al*., 2000; Lewis and Lloyd, 2012). Mature human EPO, growth hormone (GH) and G-CSF were cloned into the ribosome display construct and selections performed on the cognate receptor. Random mutagenesis libraries for EPO and G-CSF were constructed using diversity PCR random mutagenesis kit (Clontech) according to the manufacturer's instructions, using an error rate of eight nucleotides per 1000 bp. *In vitro* transcription of mRNA and *E.coli* S30 extract translation reactions were performed as previously described (Buchanan, 2012). The 100 μl translations were performed in the presence or absence of DTT at 37°C for 7 min. After translation, the ribosome complexes were diluted in room temperature selection buffer (50 mM Tris acetate (pH 7.5), 150 mM NaCl, 50 mM magnesium acetate, 0.1% Tween 20, 2.5 mg/ml heparin with the corresponding concentration of DTT and KCl used in stability selection) to a final volume of 600 μl. The ribosome complexes were divided into two samples with and without stability selection. For stability selection the 600 μl of mRNA complexes were incubated with 1 ml of HIC matrix (GE Healthcare), previously washed three times in selection buffer, for 30 min with gentle end-over-end rotation. Samples were centrifuged at 4000 × *g* for 2 min to collect the HIC matrix. The supernatant was transferred to a fresh RNAse-free tube and centrifuged for 5 min at 4°C. The ribosome complexes were incubated with human cognate receptor-Fc fusion (R&D Systems, Abingdon, UK) at 4°C for 1–2 h, followed by capture on protein G-coated magnetic beads as appropriate (Dynal Biotech, Bromborough, UK). Beads were washed five times with ice-cold selection buffer to remove non-specifically bound ribosome complexes. mRNA was eluted, purified and cDNA amplified by reverse transcription as described previously (Buchanan, 2012).

End-point PCR was performed to visualise amplification of the full-length construct in selections and to re-amplify selection outputs prior to subsequent rounds of selection. A 5 μl sample of each reverse transcription reaction was amplified with a PCR master mix (ABgene, Epsom, UK) containing 5% dimethyl sulphoxide and 0.25 μM of each primer (For 5′ ATACGATAATACGACTCACTATAGGGAGACCAC AACGG 3′; Rev 5′ CCGCACACCAGTAAGGTGTGCGGT ATCACCAGTAGCACCATTACCATTAGCAAG 3′). Thermal cycling was 94°C for 3 min, then 94°C for 30 s, 55°C for 30 s and 72°C for 1.5 min for 30 cycles, with a final step at 72°C for 5 min. PCR products were visualised by electrophoresis on an ethidium bromide stained 1% tris-acetate-EDTA agarose gel. For stability selections, PCR products were gel purified using the QiaQuick gel extraction kit (Qiagen) according to the manufacturer's instructions and re-amplified using the PCR conditions described above. PCR products were then used directly for *in vitro* transcription as described. In order to provide accurate relative quantitation of selection outputs, real-time PCR was performed using a Taqman assay targeted to regions of the tether sequence that were common to all constructs. Real-time PCR reactions were performed in an ABI 7700 (Applied Biosystems) or a Chromo4 (Genetic Research Instrumentation) in 25 μl reactions containing 12.5 μl 2× ABI Universal master mix (Applied Biosystems), 300 nM each of forward and reverse primer, 200 nM dual-labelled (5′FAM, 3′ TAMRA) probe and 5 μl reverse transcription reaction. cDNA levels were analysed by relative comparison of C_T (cycle number to threshold) values and relative quantitative value (RQV) calculated as follows: $RQV = 2^{-\text{delta } CT}$, where delta $C_T = C_T$ of the calibrator sample – C_T of a test sample. The calibrator sample should be the negative, no antigen, control.

EPO radio immunoassay stability screen

EPO variants were screened for stability using a radio immunoassay (RIA) (Jermutus *et al*., 2001). The selection output was digested with NotI and NcoI, ligated into pIVEX2.3d vector, transformed into *E.coli* TG1 cells and individual colonies picked in 96-well plates. For individual clones a linear DNA template was PCR amplified and the mRNA transcribed (Ribomax kit, Promega, following the manufacturer's instructions), purified on G25 sephadex columns and then quantified. For each variant, 10 μl S30 *in vitro* translations were set up in the presence of ^{35}S-labelled methionine, in duplicate one in no-reducing conditions and one in 10 mM DTT. The translation was stopped with 100 μl of phosphate-buffered saline (PBS) 0.05% Tween 20 with the corresponding concentration of DTT. The translation product was incubated on EPO receptor (at 1 μg/ml)-coated plates for 1 h before washing three times with PBS 0.05% Tween 20 and three times with PBS. Radioactive EPO was eluted with 0.1 M triethylamine and quantified by liquid scintillation counting. A measure of the EPO variants stability was calculated as the % residual binding = (RIA signal in 10 mM DTT/RIA signal in the absence of DTT) × 100.

EPO-accelerated stability study

EPO and EPO variant coding sequences were inserted into the pEE12.4 expression vector (Lonza Biologics) and stably transfected pools of Chinese Hamster Ovary, CHO-K1SV (Lonza Biologics) were established. Monomeric EPO proteins were purified and tested for stability. Protein samples were stored in sterile glass vials with metal crimped lids at 5, 37 and 45°C for 2 weeks. At time zero, week 1 and week 2 samples were analysed by sodium dodecyl sulphate polyacrylamide gel electrophoresis (SDS-PAGE) reducing and non-reducing conditions, absorbance, isoelectric focusing (IEF) and high-performance liquid chromatography (HPLC) (BioSep-size-exclusion chromatography [SEC]-s2000 column), to identify proportion of monomer, aggregates and breakdown products over time.

G-CSF E.coli *soluble expression*

G-CSF and G-CSF variants were expressed in pCANTAB6 vector with a C-terminal 10× His tag in *E.coli* strain HB2151 cells (Biostat Diagnostics). The 500 μl expressions were performed in triplicate in 96-well monster blocks (Greiner Bio-One) in 2× TY broth. Plates were incubated at 37°C, 600 rpm for 6 h, induced with isopropyl β-D-thiogalactoside and grown overnight in a HiGro incubator (Genemachines

Inc.). The cells were harvested by centrifugation at 2500 × *g* for 10 min and the periplasmic material was released by re-suspending the cell pellet in 200 μl of 200 mM Tris pH 8.0, 1 mM ethylendiaminetetraacetic acid, 0.5 M sucrose, 0.1% Tween at 4°C for 20 min. Cell debris was removed by centrifugation at 2500 × *g* for 10 min and the protein samples were purified on NiNTA phynexus tips (PhyNexus Inc.) following the manufacturer's instructions. The samples were run on E-PAGE™ 96 gels (Invitrogen), western blotted and detected with an anti-G-CSF antibody (R&D AF-214). Large-scale expression was performed as 400 ml cultures and periplasmic production performed as above. Protein purification was performed using an AKTA Explorer (GE Healthcare).

Proliferation assays

The biological activity of G-CSF and G-CSF variants was assessed in an OCI/AML5 cell proliferation assay. OCI/AML5 cells were obtained from Leibniz-Institut DSMZ (ACC 247) and maintained according to the supplier's protocols. Cells were washed four times in assay media (minimum essential media alpha containing 16.6% v/v foetal bovine serum) and re-suspended at a final concentration of 1×10^5 cells/ml. In triplicate G-CSF protein was diluted to the desired concentration in assay media and added to 100 μl of cells, to a final volume of 200 μl/well. Assay plates were incubated at 37°C for 72 h under 5% CO_2, 20 μl of tritiated thymidine (5 Ci/ml, NEN) added and incubated for a further 4 h. Cells were harvested and thymidine incorporation was determined using a Packard TopCount microplate scintillation counter and data analysed using Graphpad Prism software.

The biological activity of EPO and EPO variants was assessed in a TF1 cell proliferation assay. TF1 cells (R&D Systems) were maintained according to the supplier's protocols. Cells were washed four times in an assay media (RPMI-1640 with GlutaMAX, 5% v/v foetal bovine serum and 1% sodium pyruvate), re-suspended at a final concentration of 1×10^5 cells/ml. The proliferation assay was performed in triplicate as for G-CSF.

Pharmacodynamics and pharmacokinetics in normal mice

All animal studies were performed according to the Institutional Animal Care and Use Committee guidelines. Recombinant EPO was delivered via intravenous (IV) injection to CD-1 mice (Charles River) at 250 U/kg. After 48 and 72 h animals were euthanised and reticulocyte levels were determined using an ADVIA 120 haematology analyser. The study was vehicle controlled with 100 μg/ml bovine serum albumin in PBS. For pharmacokinetic (PK) analysis CD-1 mice were dose with 250 U/kg EPO IV. Serum samples were obtained at 0.5, 4, 24 and 48 h post-dose. The serum recombinant human EPO concentrations were determined with Quantikine IVD human erythropoietin kits (R&D Systems).

Structural analysis and aggregation prediction

Structural models for EPO and G-CSF and mutants were built using software programs from Accelrys Software Inc. starting from crystal structures of these proteins (Syed *et al.*, 1998; Aritomi *et al.*, 1999) as templates. Aggregation-prone regions were predicted using software tools from Accelrys Software Inc. and figures generated with Discovery Studio.

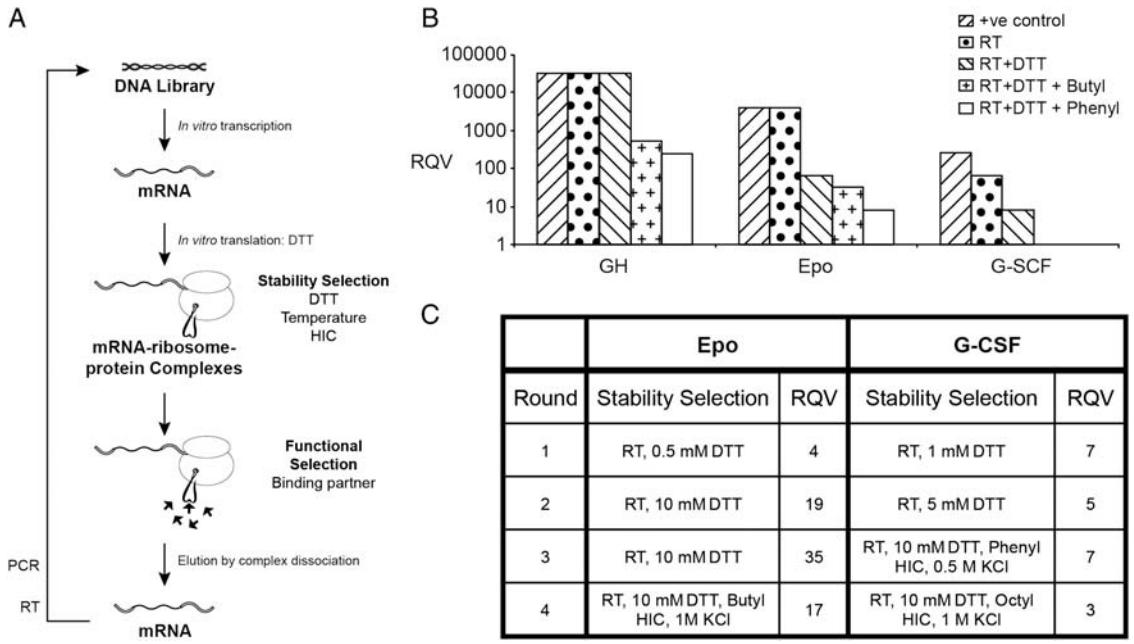

C

	Epo		G-CSF	
Round	Stability Selection	RQV	Stability Selection	RQV
1	RT, 0.5 mM DTT	4	RT, 1 mM DTT	7
2	RT, 10 mM DTT	19	RT, 5 mM DTT	5
3	RT, 10 mM DTT	35	RT, 10 mM DTT, Phenyl HIC, 0.5 M KCl	7
4	RT, 10 mM DTT, Butyl HIC, 1M KCl	17	RT, 10 mM DTT, Octyl HIC, 1 M KCl	3

Fig. 1. (**A**) Schematic of the selection cascade incorporating stability selection pressures. A library of DNA variants is first transcribed *in vitro* to mRNA. *In vitro* translation, in the presence of DTT to prevent formation of stabilising disulphide bridges in the displayed molecules, generates mRNA–ribosome–protein complexes. The complexes are selected for stability by incubation at increased temperature with DTT and HIC matrix and then for function by selection on the binding partner. mRNA is recovered by dissociation of the ribosome complexes, reverse transcribed and amplified for the next round of selection. (**B**) Impact of temperature on a cycle of ribosome display for GH, EPO and G-CSF. Selections were performed at 4°C (+ve control), room temperature (RT) in the presence of DTT and butyl or phenyl HIC matrices. The outputs were assessed by RQV, which is proportional to the amount of mRNA recovered from the selection, to enable comparison between molecules. (**C**) Stability selection conditions used for EPO and G-CSF. At each round of selection a range of stability pressures were tested. Only the selections that progressed to the next round are shown. In all cases the RQV was calculated using the no antigen control as the calibrator sample.

Results

Selection cascade based on concurrent folding and target binding

Fig. 1A shows the approach used to improve the folding properties of therapeutic proteins. Ribosome display is typically performed at 4°C to ensure the stability of the ribosome–mRNA–polypeptide complex. To test the impact of a room temperature step we performed a cycle of ribosome display with either the conventional ice-cold buffers or room temperature buffers for 30 min prior to capture on the biotinylated cognate-binding partner at 4°C. Relative quantification of the outputs by Taqman demonstrated that the room temperature step had no impact on EPO and GH outputs but significantly reduced the G-CSF output (Fig. 1B). To reveal a stability selection window, model selections were performed using concurrent stability selection pressures prior to capture on the biotinylated target at 4°C. These included (i) room temperature with DTT, (ii) room temperature, DTT and butyl HIC and (iii) room temperature, DTT and phenyl HIC (Fig. 1B). Combining room temperature and DTT made no impact on GH selection output but did provide a significant selection window for EPO and G-CSF. The addition of butyl or phenyl HIC revealed a selection window for GH, increased it for EPO and abolished the G-CSF selection window. The combination of the concurrent pressures, room temperature, DTT and HIC increased the selection window for all three molecules.

To demonstrate that protein stability and expression could be enhanced while maintaining functional activity, libraries for EPO and G-CSF were created by random mutagenesis and progressed through stability selections. Four rounds of selection were performed with increasingly stringent combinations of temperature, DTT and HIC. The selection cascade and relative enrichment are outlined in Fig. 1C. The round 4 selection outputs were cloned and screened. The EPO output was screened for improved stability and the G-CSF was screened for enhanced expression.

Enhanced G-CSF soluble expression

The G-CSF output was screened for soluble expression. In brief, the round 4 output was cloned and expressed in the periplasm of *E.coli* strain HB2151. The wild-type (WT) G-CSF and 88 variants protein were purified from the periplasm and quantified by western blot using an anti-G-CFS antibody.

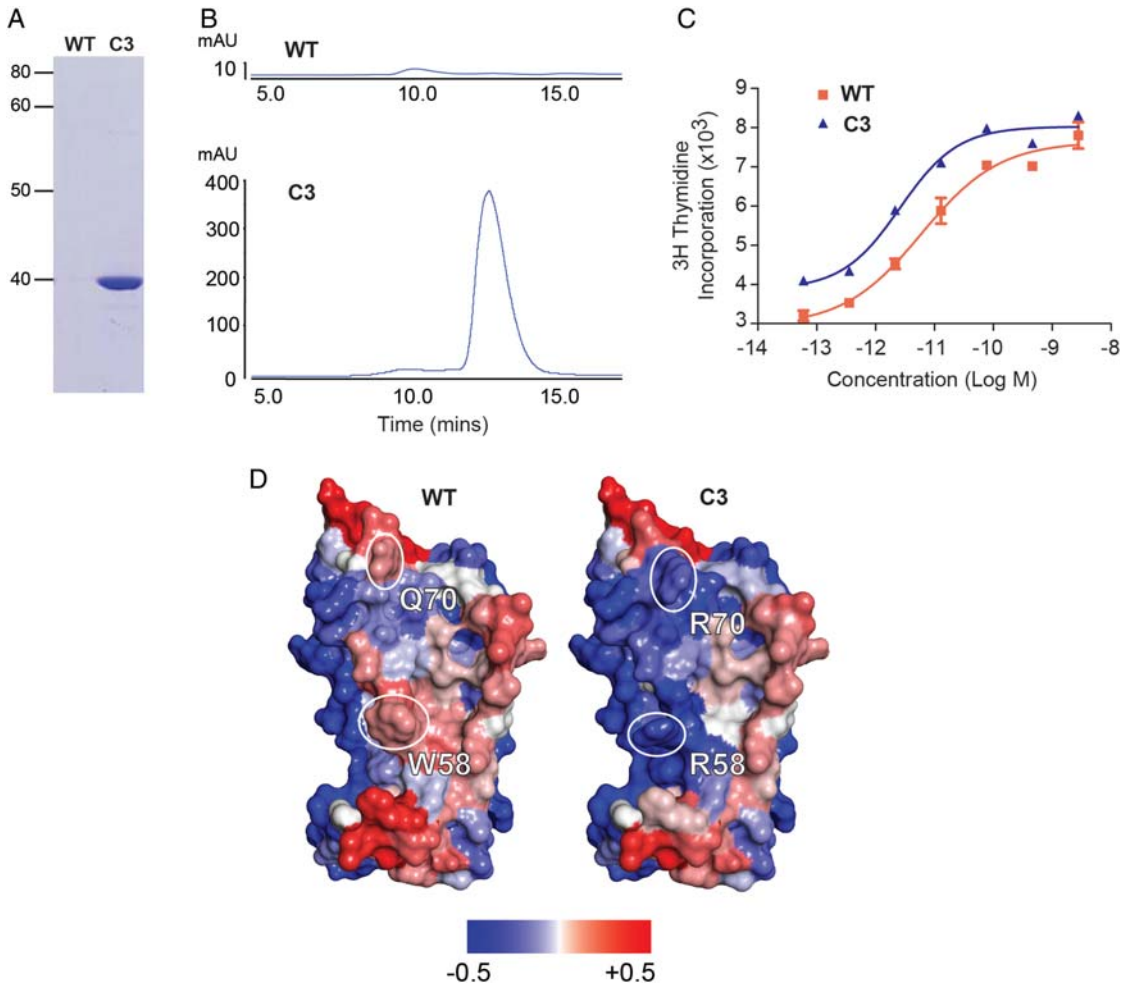

Fig. 2. Enhanced soluble *E.coli* expression of G-CSF variant C3 compared with WT. (**A**) Non-reducing SDS-PAGE gel of WT and variant C3. (**B**) SEC-HPLC traces for WT and C3. (**C**) *In vitro* potency of WT and C3 in the OCI/AML5 cell proliferation assay. (**D**) Aggregation prediction of G-CSF WT and variant C3, demonstrating a significant reduction in aggregation propensity in regions around mutated sites 58 and 70. Mutated sites 17 and 83 are not shown in this view. On the scale shown for aggregation propensity, red is more aggregation prone and blue is less aggregation prone.

From this two clones with increased proportion of monomer expression were identified (data not shown). To confirm this increase in soluble expression WT and the variant C3 expression was scaled up to 2 l and after purification were analysed by SDS-PAGE and SEC-HPLC (Fig. 2A and B). WT expression was just detectable by SEC-HPLC, quantified as 8 μg/l, the retention time equates to G-CSF dimer, which may be partially aggregated as OD 254 was higher than OD 280. C3 expressed at high levels, 8 mg/l, and was primarily monomer. Functional activity for both molecules was confirmed in a proliferation assay. C3 retained equivalent functional activity to WT with EC_{50} of 2.6 and 6 pM, respectively (Fig. 2C).

G-CSF C3 encoded four mutations relative to WT which are C17G W58R, Q70R and F83L. To gain insight into how these mutations enhance the stability and expression of G-CSF structural models were generated and used as the basis for aggregation prediction using computational tools from Accelrys Software Inc. Of the four mutations, two were predicted to significantly reduce aggregation propensity compared with WT (Fig. 2D). The W58R mutation reduces the aggregation propensity score from 2.96 to 1.28 in a 10 Å radius of position 58. The Q70R mutation reduced the aggregation propensity score from 2.55 in the WT to 2.34 in a 10 Å radius of position 70. No change in aggregation propensity was predicted at position 17 or 83. In addition, analysis of receptor-bound structures (Aritomi *et al.*, 1999; Tamada *et al.*, 2006) revealed that none of the mutated positions form part of the receptor-binding interface.

Enhanced EPO stability

The EPO output was screened in a stability RIA. In brief, variants were *in vitro* translated in the presence of ^{35}S-labelled methionine in duplicate, one in non-reducing conditions and one in 10 mM DTT. The translation mixture was incubated on an EPO receptor-coated plate, the plate was washed and radioactive EPO eluted and quantified. A surrogate measure of stability was calculated as % residual binding = (signal in 10 mM DTT/non-reducing signal) × 100. Variants with improved % residual binding were identified (Fig. 3A). To investigate if the EPO variants had enhanced stability an accelerated stability assay was performed. In brief, WT and two variants with highest % residual binding were expressed in CHO cells, purified and then incubated at 10 mg/ml in PBS at 5 and 45°C for 2 weeks. The percentage of monomer was monitored and bio activity was tested in a TF1 proliferation assay (Fig. 3B). There was a rapid and significant loss in the % monomer of WT EPO, with a concomitant rise in both aggregates and fragment. The reduction in monomer correlated with a concomitant rise in aggregate and fragment (data not shown) and a significant drop in potency. The two variants retained their monomeric nature over 2 weeks at 45°C and full bioactivity.

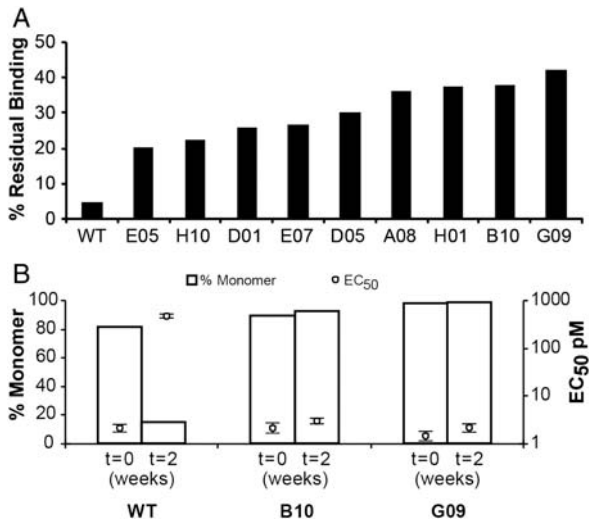

Fig. 3. Enhanced stability and retained potency of EPO variants. (**A**) Radioimmunoassay for EPO variants compared with WT. EPO binding to EPO receptor was measured in non-reducing and reducing conditions and the percentage (%) residual binding was calculated as a surrogate measure of stability. (**B**) Purified protein was assessed in an accelerated stability study. The percentage monomer was measured at time zero ($t = 0$) and 2 weeks ($t = 2$) at 5 and 45°C by SEC-HPLC. The potency of EPO samples was tested in a TF1 proliferation assay at time zero and after 2 weeks at 45°C and is shown in hollow circles as a mean of triplicate experiments.

The EPO variants contained 4–10 amino acid mutations. The variant G09 encoded four changes. Based on this a panel of single, double and triple mutants were constructed and tested in the stability RIA to explore if the changes were additive or synergistic (Fig. 4A). The individual or double point mutants delivered no significant improvement in stability as assessed by % residual binding. However, when they were combined as triple mutants or four changes as in G09 the mutations were synergistic.

To gain insight into how these mutations enhance the stability of EPO structural models were generated and used as the basis for aggregation prediction. Of the four mutations, only one was predicted to reduce aggregation propensity compared with WT (Fig. 4B). The G158E mutation reduces the aggregation propensity score from 0.78 in the parent molecule to 0.42 in the mutant. Comparison of the EPO and the G09 mutant structures suggests that E158 in the mutant may have eliminated the contribution of L155 to the aggregation propensity of this region in the folded state. No change in aggregation propensity was predicted at position 25, 27 or 139. Structural analysis of the co-complex revealed that none of the positions mutated, except for G158E in EPO, are at receptor-binding regions (Syed *et al.*, 1998). E158 in EPO may even contribute to additional hydrophobic interactions with the receptor. Thus, the mutations are not predicted to affect receptor binding or bioactivity significantly.

The *in vivo* functional potency and PK profile of EPO variants were evaluated in a normocythemic mouse model, using stimulation of immature RBCs as an indicator of bioactivity. The variants tested were potent stimulators of erythropoiesis *in vivo*, comparable to WT EPO as shown in Fig. 5A. The PK profile of EPO variant B10 was equivalent to that of WT EPO (Fig. 5B).

Discussion

This study demonstrated clearly that combining ribosome display with the appropriate selection pressures was able to improve the soluble expression level of G-CSF by 1000-fold and to significantly reduce the aggregation propensity of EPO, both of which are molecules of therapeutic interest. Stability selection using ribosome display has been demonstrated previously (Jermutus *et al.*, 2001; Matsuura and Plückthun, 2003). However, these methods were limited to one stability selection pressure or sequential stability steps.

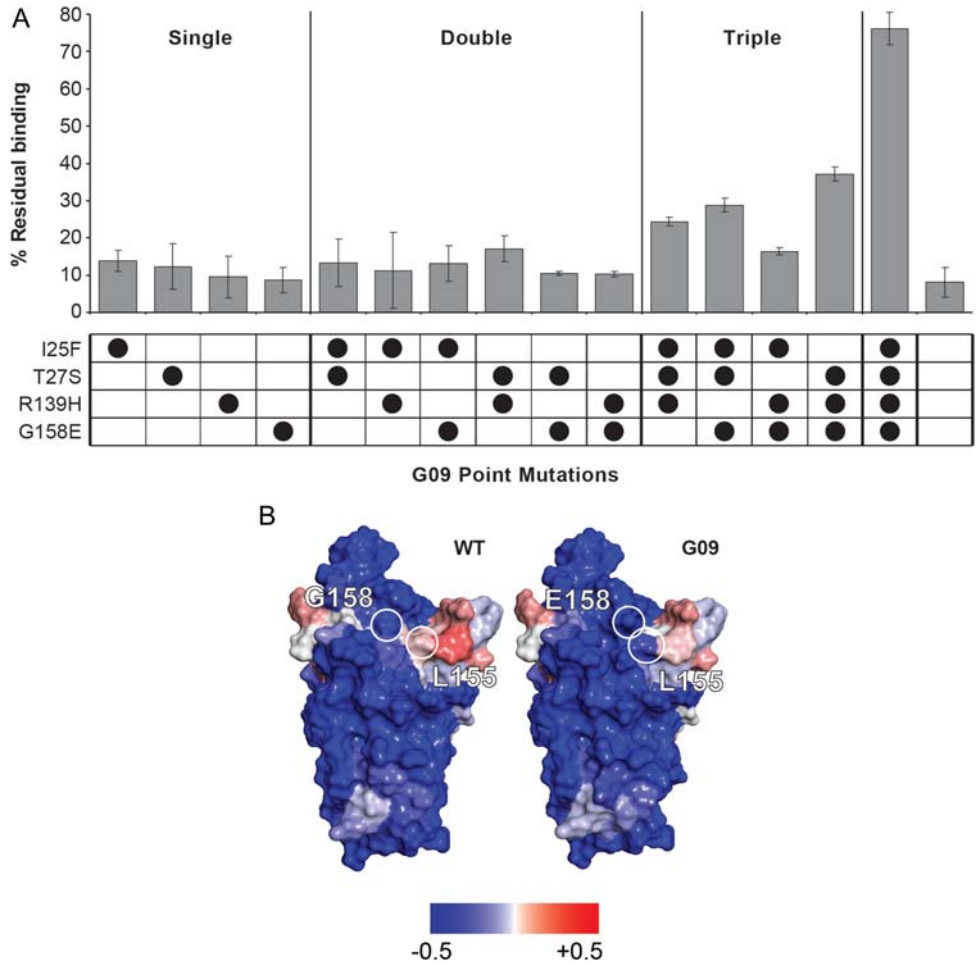

Fig. 4. (**A**) Synergistic combination of mutations. The four stability enhancing mutations in variant G09 at positions 25, 27, 139 and 158 were introduced in EPO as single, double and triple combinations. The variants were expressed and tested in the surrogate stability assay and the percentage residual binding was calculated. (**B**) Aggregation prediction for EPO WT and G09 demonstrating a slight reduction in aggregation propensity of the region involving the non-mutated site 155. This aggregation prone region is near the mutated site 158. On the scale shown for aggregation propensity, red is more aggregation prone and blue is less aggregation prone.

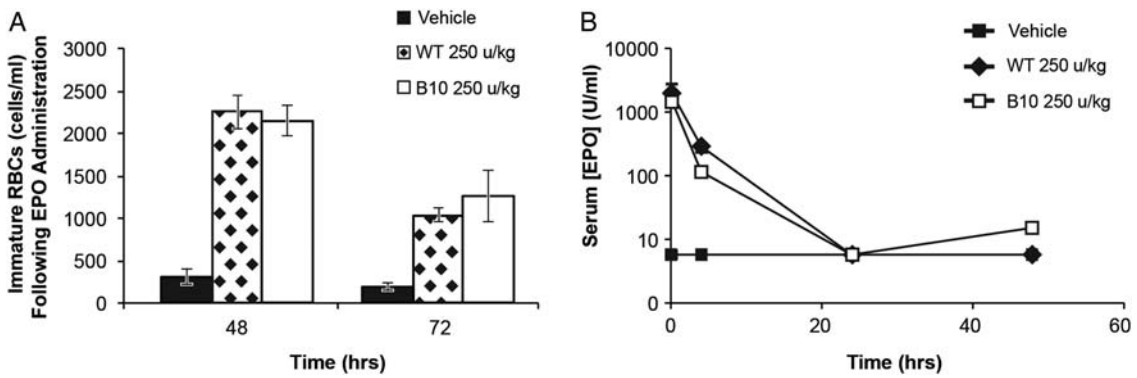

Fig. 5. (**A**) Pharmacodynamic activity of variant EPO in mice is similar to WT EPO. Groups ($n = 5$/group) of CD-1 mice were injected with a single dose of 250 U/kg IV and the number of immature RBCs was measured at 24 and 48 h. The data shown are group means of immature RBCs $\pm$ SEM. (**B**) Pharmacokinetic comparison of EPO in mice following IV administration. CD-1 mice were dosed with EPO at 250 U/kg IV.

Jermutus stabilised an antibody scFv using selections with increasing concentration of DTT. Matsuura demonstrated that ribosome display selections with HIC could selectively remove aggregation-prone peptides. This paper further develops ribosome display stability selection methods by using up to three concurrent stability selection pressures DTT, HIC and temperature in combination with selection for function. The use of individual selection pressures can limit the utility of the methodology. In the case of GH it was only the combination of three concurrent selection pressures that increased the stringency enough to reveal a selection window. Individual molecules will require a tailored selection cascade and this method enables a flexible approach to evolve protein stability.

Ribosome display is performed at 4°C to ensure the stability of the ribosome–mRNA–polypeptide complex (Hanes *et al.,* 2000). The inclusion of a 30 min room temperature step could be detrimental to the integrity of the ribosome–mRNA–polypeptide complex. Surprisingly, the complexes for GH and EPO remained intact as determined by relative quantification of the mRNA output. The room temperature step alone did cause a slight reduction in the G-CSF mRNA output. However, there was still a viable selection window over background. The addition of a temperature step has two potential advantages for stability selection. Firstly, it enables the protein folding to be in dynamic equilibrium to a greater degree than at 4°C. Secondly, it increases the utility of HIC to remove exposed hydrophobic residues in aggregation prone molecules. These stability selections were performed with *E.coli* S30 extracts. Recently, it has been reported that *in vitro* translation with purified components (PURE system) enables incubation of the ribosome–mRNA–polypeptide complex at room temperature and up to 50°C (Ueda *et al.,* 2010; Plückthun, 2012). Therefore, using the PURE system with these concurrent stability selections could further enhance the utility of ribosome display for stability evolution. This would enable a directed evolution approach to proteins with even higher thermal stability.

For both EPO and G-CSF a reduction in the aggregation propensity scores for the stable mutants was predicted. A significant reduction in aggregation propensity was predicted especially for the W58R mutation in G-CSF. The predictions suggest that reduction in aggregation propensities may have contributed to the enhancement of stability and solubility of the two proteins in their folded states. However, as the mutations include charged residues changes in protein pI and interactions with solvent should be considered in explaining the enhanced solubility and stability of the mutants as in the case of supercharged proteins (Lawrence *et al.,* 2007; Miklos *et al.,* 2012). Consistent with this notion, significant differences in both protein pI and pH for maximal stability were predicted between the EPO and the G09 mutant. The predicted values for the G09 mutant (pI = 6.59 and pH for maximal stability = 7.8) relative to EPO (pI = 8.9 and pH for maximal stability = 4.4) may have resulted in enhanced stability of this mutant at neutral pH.

The disastrous consequences of EPO-derived immunogenicity was pure red cell aplasia in patients (Casadevall *et al.,* 2002; Bennett *et al.,* 2004). The reason behind this remains unclear, but one important factor is aggregation of EPO (Schellekens and Jiskoot, 2006; McKoy *et al.,* 2008). The risk of aggregation is higher when drugs are self-administered by patients via a subcutaneous route. One strategy to reduce immunogenicity is to increase protein stability. Increased stability can (i) increase resistance to proteolysis in antigen processing cells, thus reducing presentation on major histocompatibility complex class II (So *et al.,* 1997; Thai *et al.,* 2004; Liu *et al.,* 2012) and (ii) reduce aggregation *in vivo*, which is a trigger for immunogenic response for proteins and vaccines (Rosenberg, 2006; Jiskoot *et al.,* 2012). When introducing amino acid changes in a sequence to increase stability it is important not to introduce additional T_H cell epitopes that could increase the immunogenicity of the therapeutic molecule. A T_H cell epitope screen (Epibase®) of the EPO variants G09 and B10 demonstrated that they encode the same number of strong and medium DRB1 T_H cell epitopes as WT EPO. Therefore, these EPO variants may be less immunogenic than EPO based on both increased stability and no additional T_H cell epitopes.

EPO and G-CSF were both selected for enhanced stability and retained functional activity and yet the G-CSF variant demonstrated a large improvement in soluble expression. There are a number of reports of G-CSF variants with improved stability (Ishikawa *et al.,* 1992; Bishop *et al.,* 2001; Luo *et al.,* 2002). However, all these reports use cytoplasmic expression in *E.coli* followed by refolding from inclusion bodies. There is only one report of soluble *E.coli* expression using a modified signal peptide for which no functional activity was demonstrated (Jeong and Lee, 2001). The rationale for improved soluble expression could be dependent upon improved co-translational folding, less misfolding in the cytoplasm, enhanced export, more stable intermediates or the removed cysteine at position 17. Unpaired cysteine residues are often predicted to cause aggregation. However, the cysteine side-chain of residue at position 17 is buried and is not expected to contribute to aggregation propensity in the folded state. A comparison of G-CSF WT and mutant C17A equilibrium denaturation demonstrated there was no significant difference in the stability of the molecules (Raso *et al.,* 2005). Interestingly, the same group identified that the loop encoding W58 undergoes a subtle conformational change that could be a target for protein stabilisation. The G-CSF variant C03 generated by ribosome display and directed evolution has targeted W58 and potentially increased the stability of the molecule. Further work is required to determine the molecular mechanisms for improved expression and the impact on G-CSF stability. However, both EPO and G-CSF examples demonstrate the power of directed evolution using ribosome display to address both protein function and stability concurrently.

In summary, the use of an *in vitro* evolution strategy based on concurrent stability selections with selection for function can markedly improve the drug-like properties of therapeutic proteins.

Acknowledgements

The authors would like to thank the DNA Chemistry and Tissue Culture teams at MedImmune for their invaluable support of this work and Jon Large for help in preparing figures.

Funding

This work was funded by MedImmune. Funding to pay the Open Access publication charges for this article was provided by MedImmune.

References

Arakawa,T., Philo,J.S. and Kita,Y. (2001) *Biosci. Biotechnol. Biochem.*, **65**, 1321–1327.

Aritomi,M., Kunishima,N., Okamoto,T., Kuroki,R., Ota,Y. and Morikawa,K. (1999) *Nature*, **401**, 713–717.

Baneyx,F. (1999) *Curr. Opin. Biotechnol.*, **10**, 411–421.

Banks,D.D., Scavezze,J.L. and Siska,C.C. (2009) *Biophys. J.*, **96**, 4221–4230.

Bennett,C.L., Luminari,S., Nissenson,A.R., *et al*. (2004) *N. Engl. J. Med.*, **351**, 1403–1408.

Bishop,B., Koay,D.C., Sartorelli,A.C. and Regan,L. (2001) *J. Biol. Chem.*, **276**, 33465–33470.

Buchanan,A. (2012) In Douthwaite,J.A. and Jackson,R.H. (eds), *Ribosome Display and Related Technologies: Methods and Protocols*. Humana Press, pp. 191–212.
Casadevall,N. and Mayeux,P. (2002) *Hematologie*, **8**, 90.
Chi,E.Y., Krishnan,S., Kendrick,B.S., Chang,B.S., Carpenter,J.F. and Randolph,T.W. (2003) *Protein Sci.*, **12**, 903–913.
Hanes,J. and Plückthun,A. (1997) *Proc. Natl Acad. Sci. USA*, **94**, 4937–4942.
Hanes,J., Jermutus,L. and Plückthun,A. (2000) In Abelson,J.N. and Simon,M.I. (eds), *Methods Enzymol.*. Academic Press, San Diego, pp. 404–30.
Ishikawa,M., Iijima,H., Satake-Ishikawa,R., *et al*. (1992) *Cell Struct. Funct.*, **17**, 61–65.
Jeong,K.J. and Lee,S.Y. (2001) *Protein Expr. Purif.*, **23**, 311–318.
Jermutus,L., Honegger,A., Schwesinger,F. and Hanes,J. (2001) *Proc. Natl Acad. Sci.USA*, **98**, 75–80.
Jespers,L., Schon,O., Famm,K. and Winter,G. (2004) *Nat. Biotechnol.*, **22**, 1161–1615.
Jiskoot,W., Randolph,T.W., Volkin,D.B., Middaugh,C.R., Schöneich,C., Winter,G., Friess,W., Crommelin,D.J.A. and Carpenter,J.F. (2012) *J. Pharm. Sci.*, **101**, 946–954.
Keefe,A.D. and Szostak,J.W. (2001) *Nature*, **410**, 715–718.
Lawrence,M.S., Phillips,K.J. and Liu,D.R. (2007) *J. Am. Chem. Soc.*, **129**, 10110–10112.
Lehmann,M. and Wyss,M. (2001) *Curr. Opin. Biotechnol.*, **12**, 371–375.
Lewis,L. and Lloyd,C. (2012) In Douthwaite,J.A. and Jackson,R.H. (eds), *Ribosome Display and Related Technologies: Methods and Protocols*. Humana Press, pp. 139–61.
Liu,W., Onda,M., Kim,C., Xiang,L., Weldon,J.E., Lee,B. and Pastan,I. (2012) *Protein Eng. Des. Sel.*, **25**, 1–6.
Luo,P., Hayes,R.J. and Chan,C. *et al*. (2002) *Protein Sci.*, **11**, 1218–1226.
Magliery,T.J., Lavinder,J.J. and Sullivan,B.J. (2011) *Curr. Opin. Chem. Biol.*, **15**, 443–451.
Manning,M.C., Chou,D.K., Murphy,B.M., Payne,R.W. and Katayama,D.S. (2010) *Pharm. Res.*, **27**, 544–575.
Matsuura,T. and Plückthun,A. (2003) *FEBS Lett.*, **539**, 24–28.
McKoy,J.M., Stonecash,R.E., Cournoyer,D., Rossert,J., Nissenson,A.R., Raisch,D.W., Casadevall,N. and Bennett,C.L. (2008) *Transfusion*, **48**, 1754–1762.
Miklos,A.E., Kluwe,C., Der,B.S., *et al*. (2012) *Chem. Biol.*, **19**, 449–455.
Park,S., Xu,Y., Stowell,X.F., Gai,F., Saven,J.G. and Boder,E.T. (2006) *Protein Eng. Des. Sel.*, **19**, 211–217.
Plückthun,A. (2012) In Douthwaite,J.A. and Jackson,R.H. (eds), *Ribosome Display and Related Technologies: Methods and Protocols*,.Humana Press, pp. 3–28.
Raso,S.W., Abel,J., Barnes,J.M., Maloney,K.M., Pipes,G., Treuheit,M.J., King,J. and Brems,D.N. (2005) *Protein Sci.*, **14**, 2246–2257.
Roodveldt,C., Aharoni,A. and Tawfik,D.S. (2005) *Curr. Opin. Struct. Biol.*, **15**, 50–56.
Rosenberg,A.S. (2006) *AAPS J*, **8**, 501–507.
Schellekens,H. and Jiskoot,W. (2006) *J Immunotoxicol*, **3**, 123–130.
Shusta,E.V., Kieke,M.C., Parke,E., Kranz,D.M. and Wittrup,K.D. (1999) *J. Mol. Biol.*, **292**, 949–956.
So,T., Ito,H., Koga,T., Watanabe,S. and Ueda,T. (1997) *J. Biol. Chem.*, **272**, 32136–32140.
Syed,R.S., Reid,S.W., Li,C., *et al*. (1998) *Nature*, **395**, 511–516.
Tamada,T., Honjo,E., Maeda,Y., Okamoto,T., Ishibashi,M., Tokunaga,M. and Kuroki,R. (2006) *Proc. Natl Acad. Sci. USA*, **103**, 3135–3140.
Thai,R., Moine,G., Desmadril,M., Servent,D., Tarride,J., Ménez,A. and Léonetti,M. (2004) *J. Biol. Chem.*, **279**, 50257–50266.
Thom,G., Cockroft,A.C., Buchanan,A.G., *et al*. (2006) *Proc. Natl Acad. Sci. USA*, **103**, 7619–7624.
Tokuriki,N. and Tawfik,D.S. (2009) *Curr. Opin. Struct. Biol.*, **19**, 596–604.
Ueda,T., Kanamori,T. and Ohashi,H. (2010) In Endo,Y., *et al*. (eds), *Cell-Free Protein Production: Methods and Protocols*. Humana Press, pp. 219–25.